1   # Model Sensitivity Studies of the Decrease in Atmospheric Carbon
2   # Tetrachloride

3   **Martyn P. Chipperfield[1,2], Qing Liang[3,4], Matthew Rigby[5], Ryan Hossaini[6],**
4   **Stephen A. Montzka[7], Sandip Dhomse[1], Wuhu Feng[1,8], Ronald G. Prinn[9],**
5   **Ray F. Weiss[10], Christina M. Harth[10], Peter K. Salameh[10], Jens Mühle[10],**
6   **Simon O'Doherty[5], Dickon Young[5], Peter G. Simmonds[5], Paul B. Krummel[11],**
7   **Paul J. Fraser[11], L. Paul Steele[11], James D. Happell[12], Robert C. Rhew[13], James Butler[7],**
8   **Shari A. Yvon-Lewis[14], Bradley Hall[7], David Nance[7], Fred Moore[7], Ben R. Miller[7],**
9   **James W. Elkins[7], Jeremy J. Harrison[15,16], Chris D. Boone[17], Elliot L. Atlas[18],**
10   **Emmanuel Mahieu[19]**

11   1. School of Earth and Environment, University of Leeds, Leeds, LS2 9JT, UK.
12   2. National Centre for Earth Observation, University of Leeds, LS2 9JT, UK.
13   3. NASA Goddard Space Flight Center, Atmospheric Chemistry and Dynamics, Greenbelt,
14   Maryland, USA.
15   4. Universities Space Research Association, GESTAR, Columbia, Maryland, USA.
16   5. Atmospheric Chemistry Research Group, School of Chemistry, University of Bristol, UK.
17   6. Lancaster Environment Centre, Lancaster University, UK.
18   7. National Oceanic and Atmospheric Administration, Boulder, USA.
19   8. National Centre for Atmospheric Science, University of Leeds, LS2 9JT, UK.
20   9. Massachusetts Institute of Technology, Cambridge, MA 02139 USA.
21   10. Scripps Institution of Oceanography, University of California San Diego, La Jolla,
22   California, 92093-0244 USA.
23   11. CSIRO Oceans and Atmosphere, Aspendale, Victoria, Australia.
24   12. Dept. of Ocean Sciences, University of Miami, Florida, USA.
25   13. Dept. of Geography, University of California, Berkeley, USA.
26   14. Texas A&M University, USA.
27   15. Department of Physics and Astronomy, University of Leicester, Leicester LE1 7RH, UK.
28   16. National Centre for Earth Observation, University of Leicester, Leicester LE1 7RH, UK.
29   17. Department of Chemistry, University of Waterloo, Canada.
30   18. Department of Atmospheric Sciences, University of Miami, Miami, FL, USA.
31   19. Institute of Astrophysics and Geophysics, University of Liège, Liège, Belgium.

33   **Abstract**
34   Carbon tetrachloride is an ozone-depleting substance, which is controlled by the Montreal
35   Protocol and for which the atmospheric abundance is decreasing. However, the current
36   observed rate of this decrease is known to be slower than expected based on reported CCl_4
37   emissions and its estimated overall atmospheric lifetime. Here we use a three-dimensional (3-
38   D) chemical transport model to investigate the impact on its predicted decay of uncertainties
39   in the rates at which CCl_4 is removed from the atmosphere by photolysis, by ocean uptake
40   and by degradation in soils. The largest sink is atmospheric photolysis (76% of total) but a
41   reported 10% uncertainty in its combined photolysis cross-section and quantum yield has

Atmospheric
Chemistry
and Physics
Discussions

only a modest impact on the modelled rate of CCl_4 decay. This is partly due to the limiting effect of the rate of transport of CCl_4 from the main tropospheric reservoir to the stratosphere where photolytic loss occurs. The model suggests large interannual variability in the magnitude of this stratospheric photolysis sink caused by variations in transport. The impact of uncertainty in the minor soil sink (9% of total) is also relatively small. In contrast, the model shows that uncertainty in ocean loss (15% of total) has the largest impact on modelled CCl_4 decay due to its sizeable contribution to CCl_4 loss and large uncertainty range (157 to 313 years). With an assumed CCl_4 emission rate of 39 Gg/yr, the reference simulation with best estimate of loss processes still underestimates the observed CCl_4 (overestimates the decay) over the past two decades but to a smaller extent than previous studies. Changes to the rate of CCl_4 loss processes, in line with known uncertainties, could bring the model into agreement with in situ surface and remote-sensing measurements, as could an increase in emissions to around 45 Gg/yr. Further progress in constraining the CCl_4 budget is partly limited by systematic biases between observational datasets. For example, surface observations from the NOAA network are larger than from the AGAGE network but have shown a steeper decreasing trend over the past two decades. These differences imply a difference in emissions which is significant relative to uncertainties in the magnitudes of the CCl_4 sinks.

1. Introduction

Carbon tetrachloride (CCl_4) is an important ozone-depleting substance (ODS) and greenhouse gas (GHG) (WMO/UNEP, 2014). Because of its high ozone depletion potential (ODP) it has been controlled since the 1990 London Amendment to the 1987 Montreal Protocol. Historically CCl_4 was used as a solvent, a fire retarding chemical and as a feedstock for production of chlorofluorocarbons (CFCs) and their replacements, though current production should be limited to feedstock, process agent and other essential applications (WMO/UNEP, 2014).

In response to the controls of dispersive uses under the Montreal Protocol and its adjustments and ammendments, the atmospheric burden of CCl_4 peaked at around 106 ppt (pmol/mol) in 1990, then declined at about 1 ppt/year (around 1%/year) through 2005 with indications of a faster rate of decline, around 1.3 ppt/yr, since then. Carpenter and Reimann et al. (2014) give the recent rate of decline (2011-2012) as 1.1-1.4 ppt/yr, depending on the observation network. However, despite this ongoing decline in atmospheric CCl_4 burden there is a significant discrepancy in the known CCl_4 budget. The atmospheric decline is significantly slower than would be expected based on reported production to dispersive and non-dispersive uses, and current estimates of the strength of CCl_4 sinks.

The main removal process for atmospheric CCl_4 is slow transport to the stratosphere followed by photolysis at UV wavelengths (see Burkholder and Mellouki et al., 2013). This photolysis mainly occurs in the middle stratosphere and so the rate of removal depends also on the slow transport of CCl_4 through the stratosphere by the Brewer-Dobson circulation, for which the speed can vary. The other significant sinks for CCl_4 are ocean uptake (Krysell et al., 1994) and degradation in soils (Happell and Roche, 2003; Happell et al., 2014).

Atmospheric
Chemistry
and Physics
Discussions

83 Uncertainties in the CCl_4 budget, where emissions derived from reported production
84 magnitudes underestimate the sources needed to be consistent with our understanding of CCl_4
85 loss processes and its change in atmospheric abundance, have been an issue for almost two
86 decades. These uncertainties have been highlighted in many of the 4-yearly WMO/UNEP
87 ozone assessments, including the most recent one in 2015. WMO/UNEP (2014) stated that
88 estimated sources and sinks of CCl_4 remain inconsistent with observations of its abundance.
89 The report used an overall atmospheric CCl_4 lifetime of 26 years to infer a need for 57 (40-
90 74) Gg/yr emissions of CCl_4, which greatly exceeded that expected based on reported
91 production for dispersive uses.

92 Liang et al. (2014) used a three-dimensional (3-D) chemistry-climate model (CCM) to
93 investigate possible causes for this 'budget gap' in CCl_4. They performed a series of
94 experiments with different assumptions of CCl_4 emissions and overall atmospheric lifetime.
95 In particular they used the observed interhemispheric gradient (IHG) of CCl_4 to infer the
96 magnitude of on-going emissions missing in the current inventories, with some information
97 on their distribution between the hemispheres. They inferred that the mean global emissions
98 of CCl_4 were 39 (34-45) Gg/yr and the corresponding overall CCl_4 lifetime was 35 (32-37)
99 years. In contrast their model calculated an overall atmospheric lifetime of CCl_4 of 25.8
100 years, based on a calculated partial lifetime for photolysis loss of 47 years and specified
101 partial lifetimes for ocean and soil loss of 79 and 201 years, respectively.

102 The partial lifetime of CCl_4 due to loss by photolysis was calculated in the recent SPARC
103 lifetimes report (SPARC, 2013; Chipperfield and Liang et al., 2013) using 6 chemistry-
104 climate models. The modelled steady-state CCl_4 partial lifetime for year 2000 conditions
105 varied from 41.4 years to 54.3 years with a mean of 49.9 years. The large spread in model
106 values was attributed to different circulation rates in the models; generally a faster tropical
107 upwelling circulation gave rise to a shorter lifetime. To obtain an overall recommended
108 photolysis lifetime value of 44 years, SPARC (2013) combined those model results with a
109 shorter lifetime of 40 years based on stratospheric tracer-tracer correlations and the loss of
110 CCl_4 relative to CFC-11 ($CFCl_3$).

111 Since the publication of Liang et al. (2014) there has been renewed interest in the CCl_4
112 budget gap. Rhew and Happell (2016) re-evaluated the global CCl_4 soil sink using new
113 observations and an improved land cover classification scheme. They derived the partial
114 lifetime of CCl_4 with respect to soil loss to be 375 (288-536) years. Similarly, Butler et al.
115 (2016) have also recently revised the partial lifetime of the ocean sink to be 210 (157-313)
116 years. Both of these partial lifetimes are much longer than previous estimates used in Liang et
117 al. (2014), as recommended in Carpenter and Reimann et al. (2014). The recent papers also
118 provide a revised uncertainty range which can be used to constrain model-data comparisons.

119 The aim of this paper is to quantify the magnitude of CCl_4 emissions over the recent past
120 using the most up-to-date information on the main CCl_4 loss processes. In particular, we use
121 the estimated uncertainties in the CCl_4 loss processes to further constrain the likely range of
122 emissions. We also test the results of Liang et al. (2014) using a different model of
123 atmospheric chemistry and transport which we compare to a range of available observations,
124 thereby contributing to more robust conclusions. Section 2 describes the CCl_4 observations

Atmospheric
Chemistry
and Physics
Discussions

Open Access

EGU

125   that we use and our 3-D chemical transport model. Section 3 compares our model simulations

126   with these observations and quantifies the emissions required for model-data agreement.

127   Section 3 also discusses our results in the context of other recent work. Our conclusions are

128   presented in Section 4.

129   **2. CCl$_4$ Observations and 3-D Model**

130   **2.1 NOAA and AGAGE CCl$_4$**

131   We have used surface CCl$_4$ observations from 11 National Oceanic and Atmospheric

132   Administration/Earth System Research Laboratory (NOAA/ESRL) cooperative global air

133   sampling sites (Hall et al., 2011) and 5 sites from the Advanced Global Atmospheric Gases

134   Experiment (AGAGE) network (Simmonds et al., 1998; Prinn et al., 2000; Prinn et al., 2016;

135   http://agage.mit.edu/) over 1995-2015 (**Table 1**). NOAA observations consist of paired air

136   samples collected in flasks approximately weekly, and sent to Boulder, Colorado for analysis

137   by gas chromatography with electron capture detection (GC-ECD) and are reported on the

138   NOAA-2008 scale. NOAA global and hemispheric averages are computed by weighting

139   station data by cosine of latitude. Actual NOAA station latitudes are used, except for South

140   Pole, for which we use 70.5°S. AGAGE observations are made at a 40-minute frequency

141   using GC-ECD instruments located at remote sites and are reported on the Scripps Institution

142   of Oceanography 2005 scale (SIO-05). AGAGE data were filtered to remove above-baseline

143   "pollution" events using the method outlined in O'Doherty et al. (2001) and the remaining

144   baseline mole fractions were averaged each month. AGAGE hemispheric and global averages

145   were calculated using the AGAGE 12-box model and the method described in Rigby et al.

146   (2014). Briefly, semi-hemispheric monthly-mean AGAGE baseline data were used to

147   constrain emissions with the model. Global average mole fractions were extracted from the a

148   posteriori forward model run.

149   **2.2 ACE**

150   The Atmospheric Chemistry Experiment – Fourier transform spectrometer (ACE-FTS) is on

151   the SCISAT satellite which was launched in early 2004. ACE-FTS uses the sun as a light

152   source to record limb transmission through the Earth's atmosphere (~300 km effective

153   length) during sunrise and sunset ('solar occultation'). ACE-FTS covers the spectral region

154   750 to 4400 cm^{-1} with a resolution of 0.02 cm^{-1} and can measure vertical profiles for more

155   trace species than any other satellite instrument, although it only records spectra for, at most,

156   30 occultation events per day (Bernath, 2016). Carbon tetrachloride is one of species

157   routinely available in the latest v3.5 processing, however the retrieved profiles are biased

158   high by up to ~20 – 30%.

159   Recently, an improved ACE-FTS CCl$_4$ retrieval has been devised (Harrison et al., 2016) and

160   this will form the basis for the upcoming processing version 4.0 of ACE-FTS data. This

161   preliminary retrieval, which is used here, is available for 527 occultations measured during

162   March and April 2005. The improvements include: a) new high-resolution infrared absorption

163   cross sections for air-broadened carbon tetrachloride, b) a new set of microwindows which

164   avoid spectral regions where the line parameters of interfering species do not adequately

165   calculate the measured ACE-FTS spectra, c) the addition of new interfering species missing

Atmospheric
Chemistry
and Physics
Discussions

166 from v3.5, e.g. peroxyacetyl nitrate (PAN), and d) an improved instrumental lineshape
167 designed for the upcoming v4.0 processing.

168

169 **2.3 NDACC Column CCl_4 Observations**

170 Carbon tetrachloride can also be retrieved from high-resolution infrared solar spectra
171 recorded at ground-based stations. A total column time series spanning the 1999-2015 period,
172 updated to be consistent with Rinsland et al. (2012), is available from the Jungfraujoch
173 station (Swiss Alps, 46.5ºN, 8ºE, 3580 m a.s.l.) and will be used here, but an effort is ongoing
174 to retrieve CCl_4 from other NDACC sites (Network for the Detection of Atmospheric
175 Composition Change, see http://www.ndacc.org).

176 Rinsland et al. (2012) provide a thorough description of the approach which allows the
177 retrieval of CCl_4 total columns from ground-based FTIR (Fourier Transform InfraRed) solar
178 absorption spectra. Briefly, the strong CCl_4 ν_3 band at 794 cm^{-1} is used, and a broad window
179 spanning the 785-807 cm^{-1} spectral range is fitted, accounting for main interferences by H_2O,
180 CO_2, O_3 as well as by a dozen second- and third-order absorbers. In particular, it has been
181 shown that line-mixing effects in the strong CO_2 Q-branch at 791 cm^{-1} have to be accounted
182 for and properly modelled by the retrieval algorithm when dealing with such a wide-window
183 approach. The associated error budget indicates total random and systematic uncertainties on
184 individual total column measurements of less than 7 and 11 %, respectively.

185

186 **2.4 HIPPO Data**

187 In-situ measurements of CCl_4 obtained during the HIAPER Pole-to-Pole (HIPPO) aircraft
188 mission have also been considered (Wofsy et al., 2011; Wofsy et al., 2012). HIPPO consisted
189 of a series of 5 campaigns over the Pacific basin using the NSF Gulfstream V aircraft:
190 HIPPO-1 (Jan, 2009), HIPPO-2 (Nov 2009), HIPPO-3 (Mar/Apr 2010), HIPPO-4 (Jun 2011)
191 and HIPPO-5 (Aug/Sep 2011). Across the campaigns, sampling spanned a large latitude
192 range, extending from near the North Pole to coastal Antarctica, and from the surface to ~14
193 km. Measured CCl_4 mixing ratios were derived from analysis of whole air samples using
194 GC/MS by both NOAA/ESRL and the University of Miami. Results from both laboratories
195 were provided on a scale consistent with NOAA/ESRL.

196

197 **2.5 TOMCAT 3-D Chemical Transport Model**

198 We have used the TOMCAT global atmospheric 3-D off-line chemical transport model
199 (CTM; Chipperfield, 2006) to model atmospheric CCl_4. The TOMCAT simulations were
200 forced by winds and temperatures from the 6-hourly European Centre for Medium-Range
201 Weather Forecasts (ECMWF) ERA-Interim reanalyses (Dee et al., 2011). The simulations
202 covered the period 1996 to 2016 with a horizontal resolution of 2.8° × 2.8° and 60 levels
203 from the surface to ~60 km. The model contained 8 parameterised CCl_4 tracers that evolved
204 in response to surface emissions and loss by calculated atmospheric photolysis rates and
205 specified partial lifetimes with respect to uptake by oceans or soils (see **Table 2**). Different

Atmospheric
Chemistry
and Physics
Discussions

206   tracers (CTC1-CTC8) use different specified combinations of the emission and loss processes
207   described below. Tracer CTC1 is the reference tracer with the current best estimate values of
208   the loss processes. The annually varying global emissions were derived with the global 1-box
209   model used in recent WMO Ozone Assessments (for details, see Velders and Daniel (2014)),
210   assuming a 35-year total lifetime for CCl_4, and the long-term surface observations of CCl_4
211   from the NOAA Global Monitoring Division (GMD) network (Hall et al., 2011). These
212   emissions were distributed spatially according to Xiao et al. (2010).

213   For the photolysis sink, monthly mean photolysis rates were calculated using a stand-alone
214   version of the TOMCAT/SLIMCAT stratospheric chemistry scheme and kinetic data from
215   Sander et al. (2011). Hourly model output was averaged to produce monthly mean photolysis
216   rates as a function of latitude and altitude. To assess the model sensitivity to the photolytic
217   loss, two model tracers used these rates changed by ±10%, in line with the recommended
218   combined uncertainty in cross sections and quantum yields from Sander et al. (2011). In
219   reality this will be a lower limit of uncertainty in the modelled photolysis rates because it
220   does not account for errors in the model radiative transfer code, ozone distribution etc.

221   The ocean sink was represented by specifying a partial lifetime of CCl_4 with respect to
222   removal from the surface grid boxes over the oceans. We used the recent results of Butler et
223   al. (2016) who derived this partial lifetime to be 209 (157-313) years. For the partial lifetime
224   of CCl_4 loss over soil we used the recently published values of Rhew and Happell (2016), i.e.
225   a best estimate of 375 years and an uncertainty range of 288-536 years.

226   The TOMCAT run was spun-up for 4 years and then all tracers were scaled to match
227   'observed' global mean CCl_4 values in early 1996 (based on WMO/UNEP A1 scenario
228   values, derived from an average of AGAGE and NOAA surface measurements). The model
229   was then run for a further 20 years until 2016.

230   **3. Results**

231   **3.1 Emissions**

232   **Figure 1** shows the evolution of the prescribed surface emissions in the model run (i.e. for
233   tracers CTC1-CTC7) over 1995-2015. As noted in Section 2.5, these were derived from
234   atmospheric observations and a global box model assuming a constant overall CCl_4 lifetime
235   of 35 years. For the purposes of this study, these prescribed emissions simply provide a time-
236   dependent reference input dataset for the 3D model. Comparisons of the 3D model with
237   atmospheric observations can then provide further, more detailed information on the likely
238   CCl_4 lifetime and the emissions required to match the atmospheric observations. Note the
239   inferred lifetime and emissions are model-dependent. **Figure 1** shows that the prescribed
240   emissions decrease from around 45 Gg/yr to about 35 Gg/yr with a more rapid decrease
241   between 2004 and 2009. The mean over the whole period is 39.35 Gg/yr (see dotted line).

242

Atmospheric
Chemistry
and Physics
Discussions

3.2 Comparison with Observations

244 First we compare the simulated CCl_4 tracers with observations to evaluate the performance of
245 the basic model. **Figure 2** compares model results (in green) with surface observations at 8
246 sites from the NOAA (blue line) and AGAGE (red line) networks for which CCl_4 data are
247 available. Sites where measurements are reported by both networks, i.e. Mace Head, Trinidad
248 Head, Samoa and Cape Grim, show that NOAA observations are larger than AGAGE by
249 about 5 ppt in 1996, which decreases to about 1 ppt by 2014. The panels also show global
250 mean CCl_4 values from the WMO/UNEP (2014) A1 scenario (black line) which was
251 constructed by a simple average of the global means derived with AGAGE and NOAA data,
252 and therefore typically lies between the results from the two networks at these sites. Note that
253 the TOMCAT runs were scaled globally to agree with the WMO/UNEP scenario in 1996.
254 **Figure 2** shows that CCl_4 from the TOMCAT reference tracer CTC1 decays more rapidly
255 than observed in the networks. By 2013 tracer CTC1 underestimates the WMO/UNEP
256 scenario by about 8 ppt. Note that although we are using an updated emission dataset, which
257 is derived from observations, the level of agreement also depends on the overall CCl_4 lifetime
258 specified or calculated in each model.

259 **Figure 3** compares total column CCl_4 from model run CTC1 with FTIR observations at
260 Jungfraujoch. At present this is the only ground-based station with a long-term dataset for
261 column CCl_4. Although the geographical coverage is therefore limited, the comparison does
262 allow us to test the modelled CCl_4 through the depth of the troposphere and not just at the
263 surface (as in **Figure 2**). An initial comparison between the observed and modelled columns
264 indicated a bias of about 15%, with TOMCAT lying below the FTIR data. Since the latter
265 could be affected by a systematic uncertainty of up to 10-11% (see Table 1 in Rinsland et al.,
266 2012), we allowed for a $\times 0.9$ scaling of the column amounts. **Figure 3** shows the model still
267 tends to underestimate the scaled FTIR column by about 0.05×10^{15} molecules cm^{-2} (about
268 5%). This difference is similar to that between the NOAA and AGAGE observed surface
269 mixing ratios in the 1990s and early 2000s, so this limits the extent to which we can assess
270 the consistency of the surface and column observations. Despite any disagreements in the
271 absolute amount of observed CCl_4, the relative decay rates can still be compared. The FTIR
272 column observations show a decline of 1.3×10^{13} molecules cm^{-2}/yr (1.18%/yr), which
273 compares well with modelled value (control tracer CTC1) of 1.5×10^{13} molecules cm^{-2}/yr
274 (1.36%/yr). Therefore, it appears that the model captures the observed relative decay of
275 column CCl_4 as well as the relative decline rate measured at the surface (1.1-1.2 %/yr from
276 1996-2013).

277 The HIPPO campaigns provided flask sampling of air at a wide range of latitudes from the
278 surface to about 14 km. **Figure 4** shows a comparison of the results from the analysis of
279 flasks collected during HIPPO from the surface to 1.5 km altitude from 5 campaigns from
280 January 2009 until September 2011. Also shown are results from model tracers CTC1
281 (control) and CTC8 (increased emissions), along with the monthly mean observations from
282 NOAA and AGAGE surface stations. Comparisons between the model and HIPPO
283 observations are summarised in **Table 3**. Consistent with the results from the surface
284 network, the HIPPO results show larger CCl_4 mixing ratios in the northern hemisphere

Atmospheric
Chemistry
and Physics
Discussions

285 compared to the southern hemisphere. There is some variability in the HIPPO observations
286 but this is larger in HIPPO-3 (March/April 2010), for example, compared to HIPPO-1
287 (January 2009). The HIPPO campaigns occurred when the difference between the surface
288 NOAA and AGAGE observations had decreased but are still apparent (**Figure 2** and **Figure**
289 **4**). It appears that the NOAA observations, which are larger than AGAGE, are in better
290 agreement with the HIPPO data at locations where both surface networks sampled ($\pm 1°$ of
291 latitude), but note that the HIPPO data is reported on the NOAA calibration scale. For
292 example, across all of the HIPPO campaigns, the mean bias (NOAA minus HIPPO) is < 0.1, -
293 0.1 and 0.2 ppt at MHD, SMO and CGO, respectively. Similarly, for AGAGE at these sites,
294 the mean bias is -1.7, -1.6 and -1.4 ppt, respectively. For the near-surface values plotted in
295 **Figure 4**, the model qualitatively captures the interhemispheric gradient (see Section 3.3 for
296 more discussion). Tracer CTC1 underestimates the HIPPO observations, with a mean
297 campaign bias in the range of -3.6 to -4.9% (**Table 3**). The agreement is improved by
298 assuming additional emissions in tracer CTC 8 (see also **Figure 2**), which has a smaller mean
299 bias in the range of -0.5 to -1.4%.

300 **Figure 5** shows HIPPO-TOMCAT comparisons in the upper troposphere/lower stratosphere
301 (UTLS) at 12-14 km. The model captures the latitudinal gradient in the observations,
302 including the large decreases at high latitudes in stratospheric air. This high latitude
303 agreement is worst in the northern polar region in November 2009 and the southern polar
304 region in June/July 2011 when the comparisons are likely to be affected by structure in the
305 tracer fields cause by large gradients around the polar vortex. Nevertheless, **Figure 5** shows
306 that the model performs realistically in terms of transport of CCl_4 to higher altitudes and
307 through the lower stratosphere to high latitudes.

308 Comparison with CCl_4 profiles in the stratosphere allows us to test how well the model
309 simulates the photolysis sink. **Figure 6** compares mean modelled profiles of CCl_4 with the
310 recent ACE-FTS research retrievals (Harrison et al., 2016) from March-April 2005 in three
311 latitude bands. The figure shows results from the control tracer CTC1 along with the tracers
312 CTC6 and CTC7, which have $\pm 10\%$ change in photolysis rate. Overall the model reproduces
313 the observed decay of CCl_4 in the stratosphere well, which confirms that the stratospheric
314 photolysis sink and transport are well modelled in TOMCAT, with a reasonable
315 corresponding lifetime. However, the difference between tracer CTC1 and tracers
316 CTC6/CTC7 is not large compared to the model-ACE differences. Hence, while the available
317 ACE data can confirm the basic realistic behaviour of the model in the stratosphere, they are
318 not able to evaluate the model more critically. When available over the duration of the ACE
319 mission, the full v4 retrieval will allow more comprehensive and critical comparisons over a
320 wider range of latitudes and seasons. Also, **Figure 6** illustrates the need to compare the
321 model transport separately through comparison of other tracers with different lifetimes and
322 distributions, before factoring the effect of photolytic loss of CCl_4.

323

324 **3.2 Impact of uncertainties in sinks**

325 **Figure 7** shows the partial CCl_4 photolysis lifetime diagnosed from reference tracer CTC1.
326 There is large short-term (monthly) variability in the instantaneous lifetime. Even for the

Atmospheric
Chemistry
and Physics
Discussions

annual mean lifetime there is significant interannual variability which is driven by interannual meteorological variability. The diagnosed annual mean CCl_4 lifetime over this period varies from around 39.5 years in 2010 to around 46 years in 2008. The impact of the meteorological variability was confirmed by running the model for 4 years with annually repeating meteorology from two different years (2008 and 2010). The results of these runs are shown by the + symbols, which show constant annual mean partial lifetimes but with a large (~7 year) difference. This ~7 year difference in the photolysis partial lifetime would correspond to a ~4 year difference in the overall atmospheric lifetime after combining with current best estimates of the ocean and soil sinks. This difference in overall lifetime will translate into a difference of ~6 Gg/yr in the emissions required to match the observations. Therefore, this circulation-driven variability can significantly influence top-down emissions estimates and their interannual changes. This also shows the derived mean emissions estimates will be model- and/or meteorology-dependent, and need to be treated with caution.

Table 2 shows the partial lifetimes specified (ocean and soil) or calculated (photolysis) in the model runs. The atmospheric partial lifetimes were diagnosed from monthly mean loss rates and monthly burdens, averaged over the model simulation. The partial lifetime for photolytic loss in the control tracer CTC1 is 41.9 years. This is somewhat smaller than the mean modelled partial lifetime in SPARC (2013) of 48.6 years, although consistent with the overall recommended value of 44 (36-58) years based on combined observations and models. Although two models in SPARC (2013) gave partial lifetimes around 41-42 years, the other five models gave values in the range 50.7 to 54.3. Therefore, it appears that the TOMCAT partial lifetime for loss by photolysis is at the younger end of the modelled range, which is consistent with a slightly young stratospheric age-of-air in this version of the TOMCAT/SLIMCAT model when forced with ERA-Interim reanalyses (Chipperfield 2006; Monge-Sanz et al., 2007). **Table 2** shows that, as expected, changing the magnitude of the soil and ocean sink does not affect the calculated photolysis partial lifetime.

Figure 8a shows the comparison of control model tracer CTC1 versus global mean surface observations, along with model sensitivity tracers CTC2 and CTC3 with minimum/maximum estimates for the ocean sink. This global comparison of tracer CTC1 shows similar behaviour to the individual stations in **Figure 2**; the control run slightly overestimates the observed rate of decay (for the level of emissions assumed). The uncertainty in the ocean sink has a large relative impact on the decay rate of CCl_4, relative to the mismatch with the AGAGE and NOAA datasets.

Figure 8b is a similar plot which uses model tracers CTC4 and CTC5 to investigate the impact of uncertainty in the soil loss rate. Here the impact on the modelled CCl_4 decay rate is relatively small due to the relatively long lifetime of CCl_4 with respect to loss by soils.

Figure 8c shows the effect of a ±10% change in photolysis rate on the modelled CCl_4 decay using runs CTC6 and CTC7. Note that the diagnosed atmospheric lifetimes in these two runs change by a lot less than 10% (e.g. 41.9 years to 43.5 years; 3.8% - see **Table 2**). This is due to compensation in the modelled chemical loss rates in the stratosphere ($J[CCl_4]$). A faster photolysis rate J will decrease the concentration of CCl_4, leading a partial cancellation in the product. This would be a property of any source gas with a stratospheric sink and large

Atmospheric
Chemistry
and Physics
Discussions

369   tropospheric reservoir. This partial cancellation in the stratospheric loss rate means that
370   uncertainty in the ocean sink still dominates. This is likely to be the case even with a much
371   larger assumed uncertainty in the modelled photolysis rates (e.g. ±20%).

372   **Figure 8d** shows the results from tracer CTC8 which assumes 15% larger emissions than
373   tracer CTC1. This increase in emissions (to a mean of around 45 Gg/yr) brings the model in
374   closer agreement with the rates of decay seen in the surface networks, especially that depicted
375   by the mean of NOAA and AGAGE observations. Over the period 1996-2015, the slope of
376   the linear fits to the lines for tracers CTC1 and CTC8 are -1.31 ppt/yr and -1.15 ppt/yr,
377   respectively. This 0.16 ppt/yr difference in slope corresponds to a difference in emissions of 6
378   Gg/yr between the two tracers (**Table 2**). The linear fits to the global mean NOAA and
379   AGAGE lines in **Figure 8d** over the same period are -1.15 ppt/yr and -1.01 ppt/yr,
380   respectively, although it should be noted that the AGAGE variation is not linear over this
381   timeframe. Nevertheless, this 0.14 ppt/yr difference in the mean slope from the two surface
382   networks (equivalent to ~5 Gg/yr emissions) is significant when compared to the magnitude
383   of the emissions needed to fit the observations under different lifetime assumptions.
384   Therefore, resolving this issue of the absolute difference in the concentrations reported by the
385   two networks will be important for a detailed quantification of the CCl_4 budget.

386   **Figure 8** shows that current uncertainty in the CCl_4 sinks could account for some, but
387   probably not all, model-observation differences noted above and that better quantification of
388   the ocean sink is important. Despite being the most important overall sink, uncertainty in
389   stratospheric photolysis is not that important, although it should be noted that the analysis
390   presented in **Figure 8** does not take account of uncertainties in model transport and the
391   methodology for calculating photolysis rates. Alternatively, model-observation agreement
392   could also be closed by an increase in emissions and our current best estimate of the partial
393   CCl_4 lifetimes would require emissions of around 45 Gg/yr for TOMCAT.

394

3.3 Interhemispheric gradient

396   **Figure 9** shows the observed interhemispheric gradient (IHG) in CCl_4 derived from the
397   NOAA and AGAGE networks along with results from model tracer CTC1. The observations
398   show that the IHG decreased from about 1.5 – 2.0 ppt around 2002 to 1.0 – 1.5 ppt around
399   2010. Although both networks show this behaviour, the IHG from the NOAA network is
400   persistently larger by about 0.3 ppt compared to the AGAGE network. In the early part of the
401   period shown, i.e. 2002 – 2005, there is not much correspondence between the variations seen
402   in the two observational records. The NOAA results, which are derived directly from the
403   station observations, show more variability that the AGAGE results which are derived from a
404   12-box model. Around 2006 -2009 the observations do tend to track each other and display a
405   similar seasonal cycle. The modelled IHG also shows a decreasing trend from around 2002
406   until 2012. However, the modelled IHG shows a regular annual cycle which does not match
407   the observations. In the middle part of the period, when there is a discernible annual cycle in
408   the IHG observed by both networks, the modelled annual cycle is out of phase. We have
409   investigated whether the sparse sampling of the NOAA and AGAGE networks may be

Atmospheric
Chemistry
and Physics
Discussions

410 responsible for some of the differences between the observations and with the model. **Figure**
411 **9** shows results of the model tracer CTC1 sampled like the AGAGE and NOAA networks
412 (i.e. at the locations give in **Table 1**). Compared to using the whole model hemispheric grid,
413 sampling at the station locations only changes the IHG slightly; for example the IHG sampled
414 at the AGAGE sites is about 0.3 ppt larger than that sampled at the NOAA sites, which is in
415 the opposite sense to the differences in the observations. However, the modelled annual cycle
416 is still out of phase with the observations in the 2006-2010 period. Some information on the
417 CCl_4 IHG is also given by the comparison with HIPPO data in **Figure 4** and **Table 3**. Over
418 the course of the campaigns, which sample air over the Pacific, the IHG based on the HIPPO
419 sampling varies from 1.0 ppt in HIPPO-3 to 1.6 ppt in HIPPO-5. This variation reflects
420 seasonal variability rather than any long-term trend. **Figure 9** shows that the model does not
421 reproduce the timing of this variation.

422 Overall, **Figure 9** shows that there are still details in the CCl_4 IHG that merit further
423 investigation. There are limitations of the TOMCAT model setup used in this study. The
424 assumed emissions distribution (from Xiao et al., (2010)) are likely not a good representation
425 of reality. The Xiao et al. (2010) emissions are based on population densities while more
426 recent regional inversion studies suggest that CCl_4 emissions originate mainly from chemical
427 industrial regions and are not linked to major population centres (Vollmer et al., 2009; Hu et
428 al., 2016; Graziosi et al., 2016). This will affect the model IHG, especially when sampled at
429 the limited surface station locations of either network. Also, the model does not have a
430 seasonally or spatially varying ocean sink which is likely to contribute to the poor agreement.
431 An accurate simulation of the CCl_4 IHG and its time variations remains as an important way
432 to test for our understanding of the CCl_4 budget.

433 **4. Conclusions**

434 We have used the TOMCAT three-dimensional (3-D) chemical transport model to investigate
435 the rate of decay of atmospheric CCl_4. In particular we have studied the impact of
436 uncertainties in the rates of CCl_4 removal by photolysis, deposition to the ocean and
437 deposition to the soils on its predicted decay. The model results have been compared with
438 surface-based in-situ and total column observations, aircraft measurements, and the available
439 satellite profiles.

440 Using photochemical data from Sander et al. (2010), and lifetimes for removal by the ocean
441 and soils of 209 years and 375 years, respectively, the model shows that main sinks
442 contribute to CCl_4 loss in the following proportions: photolysis 76%, ocean loss 15% and soil
443 loss 8%. A 10% uncertainty in the combined photolysis cross section and quantum yield has
444 only a modest impact on the rate of modelled CCl_4 decay, partly due to the limiting effect of
445 the rate of transport of CCl_4 from the main tropospheric reservoir to the stratosphere where
446 photolytic loss occurs. The model shows uncertainties in ocean loss has the largest impact on
447 modelled CCl_4 decay due to its significant contribution to the loss and large uncertainty range
448 (157 to 313 years). The impact of uncertainty in the minor soil sink is relatively small.

449 With an assumed CCl_4 emission rate of 39 Gg/yr the control model with best estimate of loss
450 processes still underestimates the observed CCl_4 over the past two decades (i.e. overestimates

Atmospheric
Chemistry
and Physics
Discussions

the atmospheric decay). Changes to the CCl_4 loss processes, in line with known uncertainties, could bring the model into agreement with observations, as could an increase in emissions to around 45 Gg/yr. Our results are consistent with those of Liang et al. (2014) who used different combinations of emission estimates and lifetimes to obtain good agreement between their 3-D model and CCl_4 observations. For example, their model run C used emissions of 50 Gg/yr with an overall lifetime of 30.7 years. Here we find a need for smaller mean emissions due to our larger overall CCl_4 lifetime, which in turn is due to updated estimates of the ocean and soil sinks. We note that as TOMCAT calculates a smaller partial photolysis lifetime compared to some other 3-D models (see SPARC, 2013; Chipperfield et al., 2014), the required emissions could be slightly less than suggested by our simulations.

From a model point of view, improved knowledge of the CCl_4 emissions required to reproduce observations will depend on better quantification of the modelled partial atmospheric lifetime. Although uncertainties in the photochemical data are small, there are model-dependent parameterisations of transport and radiative transfer which can affect the atmospheric partial lifetime significantly. Studies with multiple 3-D models could be used to address this.

Atmospheric
Chemistry
and Physics
Discussions

491 **References**

492 Burkholder, J.B., W. Mellouki, et al.: Evaluation of Atmospheric Loss Processes, Chap. 3 of
493   *SPARC Report on the Lifetimes of Stratospheric Ozone-Depleting Substances, Their*
494   *Replacements, and Related Species*, M. Ko, P. Newman, S. Reimann, S. Strahan (Eds.),
495   SPARC Report No. 6, WCRP-15/2013, 2013.

496 Bernath, P. F.: The Atmospheric Chemistry Experiment (ACE), *J. Quant. Spectrosc. Radiat.*
497   *Transf.*, (in press), doi:10.1016/j.jqsrt.2016.04.006, 2016.

498 Butler, J. H., S. A. Yvon-Lewis, J. M. Lobert, D. B. King, S. A. Montzka, J. L. Bullister, V.
499   Koropalov, J. W. Elkins, B. D. Hall, L. Hu, and Y. Liu: A comprehensive estimate for
500   loss of atmospheric carbon tetrachloride (CCl_4) to the ocean, *Atmos. Chem. Phys.*,
501   (submitted), doi:10.5194/acp-2016-311, 2016.

502 Carpenter, L.J., S. Reimann, J.B. Burkholder, C. Clerbaux, B.D. Hall, R. Hossaini, J.C.
503   Laube, and S.A. Yvon-Lewis: Ozone-Depleting Substances (ODSs) and Other Gases of
504   Interest to the Montreal Protocol, Chapter 1 in *Scientific Assessment of Ozone Depletion:*
505   *2014,* Global Ozone Research and Monitoring Project – Report No. 55, World
506   Meteorological Organization, Geneva, Switzerland, 2014.

507 Chipperfield, M.P., New version of the TOMCAT/SLIMCAT off-line chemical transport
508   model: Intercomparison of stratospheric tracer experiments. *Q. J. R. Meteorol Soc.,* 132,
509   1179–1203, 2006.

510 Chipperfield, M.P., Q. Liang, et al.: Evaluation of Atmospheric Loss Processes, Chap. 5 of
511   *SPARC Report on the Lifetimes of Stratospheric Ozone-Depleting Substances, Their*
512   *Replacements, and Related Species*, M. Ko, P. Newman, S. Reimann, S. Strahan (Eds.),
513   SPARC Report No. 6, WCRP-15/2013, 2013.

514 Chipperfield, M. P., Q. Liang, S. E. Strahan, O. Morgenstern, S. S. Dhomse, N. L. Abraham,
515   A. T. Archibald, S. Bekki, P. Breasicke, G. Di Genova, E. F. Fleming, S. C. Hardiman, D.
516   Iachetti, C. H. Jackman, D. E. Kinnison, M. Marchand, G. Pitari, J. A. Pyle, E. Rozanov,
517   A. Stenke, F. Tummon, Multi-model estimates of atmospheric lifetimes of long-lived
518   Ozone-Depleting-Substances: Present and future, *J. Geophys. Res.,* 119,
519   doi:10.1002/2013JD021097, 2014.

520 Dee, D.P., et al.: The ERA-Interim reanalysis: Configuration and performance of the data
521   assimilation system. *Q. J. R. Meteorol. Soc.,* 137, 553–597, 2011.

522 Graziosi, F., J. Arduini, P. Bonasoni, F. Furlani, U. Giostra, C. Lunder, A. J. Manning, A.
523   McCulloch, S. J. O'Doherty, P. G. Simmonds, S. Reimann, M. K. Vollmer, and M.
524   Maione: Emissions of carbon tetrachloride (CCl_4) from Europe, *Atmos. Chem. Phys.*,
525   (submitted), doi:10.5194/acp-2016-326, 2016.

526 Hall, B. D., G. S. Dutton, D. J. Mondeel, J. D. Nance, M. Rigby, J. H. Butler, F. L. Moore, D.
527   F. Hurst, and J. W. Elkins: Improving measurements of SF_6 for the study of atmospheric
528   transport and emissions, *Atmos. Meas. Tech.*, 4, 2441–2451, doi:10.5194/amt-4-2441-
529   2011, 2011.

530 Happell, J.D., and M.P. Roche: Soils: a global sink of atmospheric carbon tetrachloride,
531   *Geophys. Res. Lett.*, 30, 1088, doi:10.1029/2002GL015957, 2003.

Atmospheric
Chemistry
and Physics
Discussions

532   Happell, J.D., Y. Mendoza, K. Goodwin: A reassessment of the soil sink for atmospheric
533   carbon tetrachloride based on flux chamber measurements., *J. Atmos. Chem.*, 71, 113-
534   123, 2014.

535   Harrison, J.J., C.D. Boone, and P.F. Bernath: New and improved infrared absorption cross
536   sections and ACE-FTS retrievals of carbon tetrachloride (CCl_4), *J. Quant. Spectrosc.*
537   *Radiat. Transf.*, (in press), doi:10.1016/j.jqsrt.2016.04.025, 2016.

538   Hu, L., S.A. Montzka, B.R. Miller, A.E. Andrews, J.B. Miller, S.J. Lehman, C. Sweeney, S.
539   Miller, K. Thoning, C. Siso, E. Atlas, D. Blake, J.A. de Gouw, J.B. Gilman, G. Dutton, J.
540   W. Elkins, B.D. Hall, H. Chen, M.L. Fischer, M. Mountain, T. Nehrkorn, S.C. Biraud, F.
541   Moore, and P.P. Tans: Continued emissions of carbon tetrachloride from the U.S. nearly
542   two decades after its phase-out for dispersive uses, *Proc. Natl. Acad. Sci.*, 113, 2880-
543   2885, doi:10.1073/pnas.1522284113, 2016.

544   Krysell, M., E. Fogelqvist and T. Tanhua: Apparent removal of the transient tracer carbon
545   tetrachloride from anoxic seawater, *Geophys. Res. Lett.*, 21, 2511-2514,
546   doi.1029/94GL02336, 1994.

547   Liang, Q., P.A. Newman, J.S. Daniel, S. Reimann, B.D. Hall, G. Dutton, and L.J.M.
548   Kuijpers: Constraining the carbon tetrachloride (CCl_4) budget using its global trend and
549   inter-hemispheric gradient, *Geophys. Res. Lett.*, 41, 5307–5315,
550   doi:10.1002/2014GL060754, 2014.

551   Monge-Sanz, B., M.P. Chipperfield, A. Simmons and S. Uppala: Mean age of air and
552   transport in a CTM: Comparison of different ECMWF analyses, *Geophys. Res. Lett.*, 34,
553   L04801, doi:10.1029/2006GL028515, 2007.

554   O'Doherty, S., P.G.Simmonds, D.M. Cunnold, H.J. Wang, G.A. Sturrock,P.J. Fraser, D.
555   Ryall, R.G. Derwent, R.F.Weiss,P.Salameh, B.R.Miller and R.G.Prinn: In situ chloroform
556   measurements at Advanced Global Atmospheric Gases Experiment atmospheric research
557   stations from 1994 to 1998, *J. Geophys. Res.*, 106, 20,429–20,444,
558   doi:10.1029/2000JD900792, 2001.

559   Prinn, R., Weiss, R., Fraser, P., Simmonds, P., Cunnold, D., Alyea, F., O'Doherty, S.,
560   Salameh, P., Miller, B., and Huang, J.: A history of chemically and radiatively important
561   gases in air deduced from ALE/GAGE/AGAGE, *J. Geophys. Res.*, 105, 17,751-17,792,
562   2000.

563   Prinn, R. G., R.F. Weiss, P.J. Fraser, P.G. Simmonds, D.M. Cunnold, S. O'Doherty, P. K.
564   Salameh, L.W. Porter, P.B. Krummel, R H.J. Wang, B.R. Miller, C. Harth, B.R. Greally,
565   F. A. Van Woy, L.P. Steele, J. Mühle, G.A. Sturrock, F.N. Alyea, J. Huang and D.E.
566   Hartley: The ALE / GAGE AGAGE Network, Carbon Dioxide Information Analysis
567   Center (CDIAC), Oak Ridge National Laboratory (ORNL), U.S. Department of Energy
568   (DOE), 2016.

569   Rhew, R.C., and J.D. Happell: The atmospheric partial lifetime of carbon tetrachloride with
570   respect to the global soil sink, *Geophys. Res. Lett.*, 43, 2889-2895,
571   doi:1002/2016GL067839, 2016.

572   Rigby, M., Prinn, R. G., O'Doherty, S., Miller, B. R., Ivy, D., Mühle, J., Harth, C. M.,
573   Salameh, P. K., Arnold, T., Weiss, R. F., Krummel, P. B., Steele, L. P., Fraser, P. J.,

Atmospheric
Chemistry
and Physics
Discussions

574   Young, D. and Simmonds, P. G.: Recent and future trends in synthetic greenhouse gas
575   radiative forcing, *Geophys. Res. Lett.*, 41, 2623–2630, doi:10.1002/2013GL059099, 2014.
576   Rinsland, C. P., E. Mahieu, P. Demoulin, R. Zander, C. Servais and J.-M. Hartmann:
577   Decrease of the carbon tetrachloride (CCl_4) loading above Jungfraujoch, based on high
578   resolution infrared solar spectra recorded between 1999 and 2011, *J. Quant. Spectrosc.*
579   *Radiat. Transf.*, 113, 1322–1329, doi:10.1016/j.jqsrt.2012.02.016, 2012.
580   Sander, S.P., et al.: Chemical Kinetics and Photochemical Data for Use in Atmospheric
581   Studies Evaluation Number 17. *JPL Publication* **10-6**, Jet Propulsion Laboratory,
582   Pasadena, USA, 2011.
583   Simmonds, P.G., D.M. Cunnold, R.F. Weiss, R.G. Prinn, P.J. Fraser, A. McCulloch, F.N.
584   Alyea, and S. O'Doherty: Global trends and emission estimates of carbon tetrachloride
585   ($CCl4$) from in-situ background observations from July 1978 to June 1996, *J. Geophys.,*
586   *Res.*, 103, 16,017-16,028, 1998.
587   SPARC, Lifetimes of stratospheric ozone-depleting substances, their replacements and
588   related species, SPARC Report no 6, WCRP-15/32013, 2013.
589   Velders, G.J.M., and J. S. Daniel: Uncertainty analysis of projections of ozone-depleting
590   substances: Mixing ratios, EESC, ODPs, and GWPs, *Atmos. Chem. Phys.*, 14, 2757–
591   2776, doi:10.5194/acp-14-2757-2014, 2014.
592   Vollmer, M.K., L.X. Zhou, B.R. Greally, S. Henne, B. Yao, S. Reimann F. Stordal, D.M.
593   Cunnold, X. C. Zhang, M. Maione, F. Zhang, J. Huang and P. G. Simmonds: Emissions
594   of ozone-depleting halocarbons from China, *Geophys. Res. Lett.,* 36, L15823,
595   doi:10.1029/2009GL038659, 2009.
596   WMO, Scientific Assessment of Ozone Depletion: 2014, Global Ozone Research and
597   Monitoring Project—Report No. 55, 416 pp., Geneva, Switzerland, 2014.
598   Wofsy, S.C., et al.: HIAPER Pole-to-Pole Observations (HIPPO): fine-grained, global-scale
599   measurements of climatically important atmospheric gases and aerosols, *Phil. Trans. R.*
600   *Soc. A*, 369, 2073-2086, doi:10.1098/rsta.2010.0313, 2011.
601   Wofsy, S.C., et al.: HIPPO Combined Discrete Flask and GC Sample GHG, Halo-,
602   Hydrocarbon Data (R_20121129). Carbon Dioxide Information Analysis Center, Oak
603   Ridge National Laboratory, Oak Ridge, Tennessee, U.S.A.
604   http://dx.doi.org/10.3334/CDIAC/hippo_012 (Release 20121129), 2012.
605   Xiao, X., R.G. Prinn, P.J. Fraser, R.F. Weiss, P.G. Simmonds, S. O'Doherty, B.R. Miller,
606   P.K. Salameh, C.M. Harth, P.B. Krummel, A. Golombek, L.W. Porter, J.H. Butler, J.W.
607   Elkins, G.S. Dutton, B.D. Hall, L.P. Steele, R.H.J. Wang and D.M. Cunnold:
608   Atmospheric three-dimensional inverse modeling of regional industrial emissions and
609   global oceanic uptake of carbon tetrachloride, *Atmos. Chem. Phys.*, 10, 10,421–10,434,
610   doi:10.5194/acp-10-10421-2010, 2010.
611

Atmospheric
Chemistry
and Physics
Discussions

612 **Tables**

613

614 **Table 1**. List of NOAA and AGAGE stations which provided CCl_4 observations.

Site Code	Site Name	Latitude (°N)	Longitude (°E)	Altitude (km)	Network
ALT	Alert, Canada	82.5	-62.5	0.2	NOAA
BRW	Barrow, USA	71.3	-156.6	0.01	NOAA
MHD	Mace Head, Ireland	53.3	-9.9	0.01	NOAA/AGAGE
NWR	Niwot Ridge, USA	40.1	-105.6	3.5	NOAA
THD	Trinidad Head, USA	41.1	-124.1	0.1	NOAA/AGAGE
KUM	Cape Kumukahi, USA	19.5	-154.8	0.02	NOAA
MLO	Mauna Loa, USA	19.5	-155.6	3.4	NOAA
RPB	Ragged Point, Barbados	13.2	-59.4	0.02	AGAGE
SMO	Tutuila, American Samoa	-14.3	-170.6	0.04	NOAA/AGAGE
CGO	Cape Grim, Australia	-40.7	144.7	0.09	NOAA/AGAGE
PSA	Palmer Station, USA	-64.9	-64.0	0.01	NOAA
SPO	South Pole, USA	-90.0	0	2.81	NOAA

615

616 **Table 2**. Summary of the TOMCAT 3-D CTM simulated CCl_4 tracers.

Tracer	Emissions (Gg/yr)[b]	Atmospheric Loss Photolysis		Surface Loss Partial Lifetimes (years)		Overall Lifetime (years) [a]
		Photochemical Data	Partial Lifetime[a]	Ocean	Soil	
CTC1	39.35	JPL	41.9	210	375	31.9
CTC2	39.35	JPL	41.8	157	375	30.4
CTC3	39.35	JPL	41.9	313	375	33.7
CTC4	39.35	JPL	41.9	210	288	31.5
CTC5	39.35	JPL	41.9	210	536	32.4
CTC6	39.35	0.9×JPL	43.5	210	375	32.9
CTC7	39.35	1.1×JPL	40.4	210	375	31.1
CTC8	45.25	JPL	41.9	210	375	32.0

617 (a). Overall and photolysis partial lifetimes for each tracer calculated from model burden and
618 loss rates.
619 (b). Mean of interannually varying emissions from 1996-2015 (see **Figure 1**).
620

621

622 **Table 3.** Summary of model-measurement comparisons for boundary layer (surface – 1.5

623 km) CCl_4 observations during HIPPO aircraft missions.

TOMCAT CCl_4 Tracer	Mean Bias (model – obs.) (ppt)	Mean Bias (model – obs.) (%)	Observed hemispheric gradient (ppt)	Modelled hemispheric gradient (ppt)	Correlation coefficient (r)
HIPPO-1 (Jan 2009)					
CTC1	-3.2	-3.6	1.1	1.6	0.8
CTC8	-0.4	-0.5	1.1	1.8	0.8
HIPPO-2 (Nov 2009)					
CTC1	-3.4	-3.8	1.3	1.4	0.6
CTC8	-0.5	-0.6	1.3	1.6	0.6
HIPPO-3 (Mar/Apr 2010)					
CTC1	-3.8	-4.3	1.0	1.6	0.5
CTC8	-0.9	-1.0	1.0	1.8	0.5
HIPPO-4 (Jun/Jul 2011)					
CTC1	-4.3	-4.9	1.4	1.1	0.6
CTC8	-1.2	-1.4	1.4	1.2	0.6
HIPPO-5 (Aug/Sep 2011)					
CTC1	-3.9	-4.5	1.6	1.0	0.7
CTC8	-0.9	-1.0	1.6	1.2	0.7

624

625 **Figures**

626
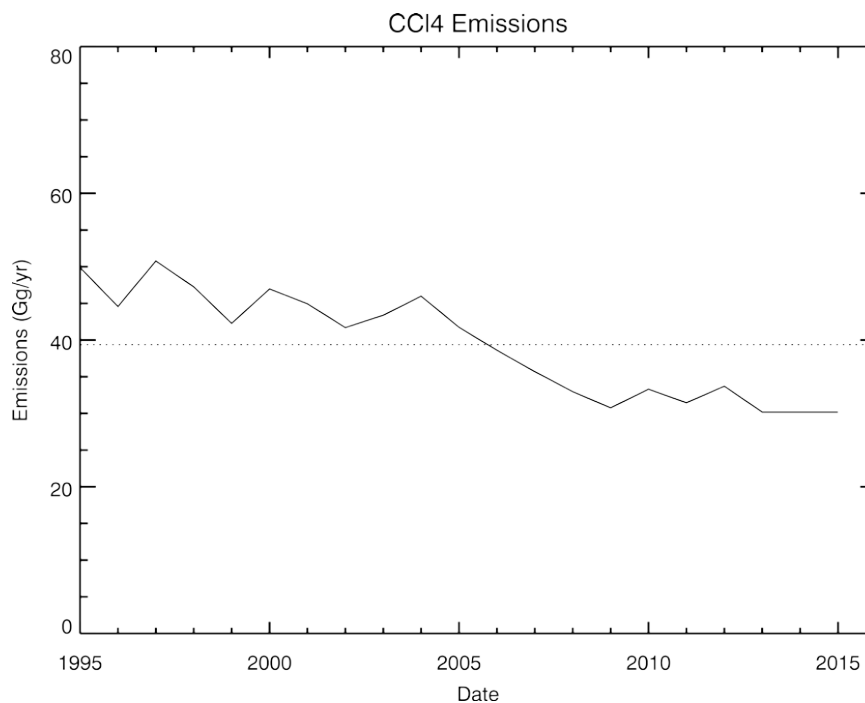
627

628 **Figure 1.** Time variation of global annual emissions (Gg/yr) derived from measured global
629 atmospheric changes and a global box model (solid line). The emission record was used for
630 the standard TOMCAT model experiments. The mean emissions over the period 1996-2015
631 are 39.35 Gg/yr (indicated by dotted line).

632

Atmospheric
Chemistry
and Physics
Discussions
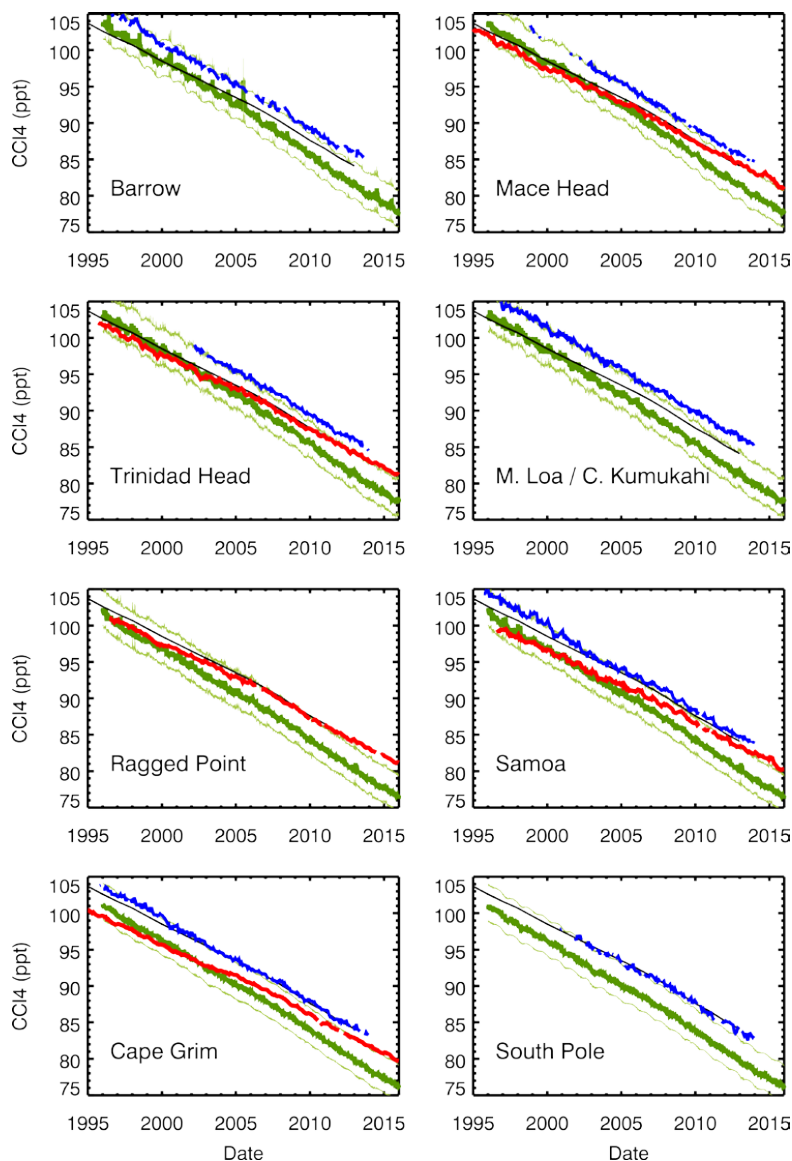
Figure 2. Comparison of modelled surface CCl_4 concentration (ppt) with observations at 8 stations in the AGAGE (red line) or NOAA (blue line) networks. Also shown is the CCl_4 global mean surface mixing ratio from WMO/UNEP (2014) scenario A1 (black line). The dark green line shows model control tracer CTC1 and light green lines show this tracer CTC1 line displaced by +3 and –2 ppt to aid comparisons with the slope of the NOAA and AGAGE observations. This range is arbitrary but indicates the how the model line would be displaced if the CTC1 tracer had been initialised to agree with either the NOAA or AGAGE global mean CCl_4 abundance in 1996.

Atmospheric
Chemistry
and Physics
Discussions

Open Access

EGU

643

644
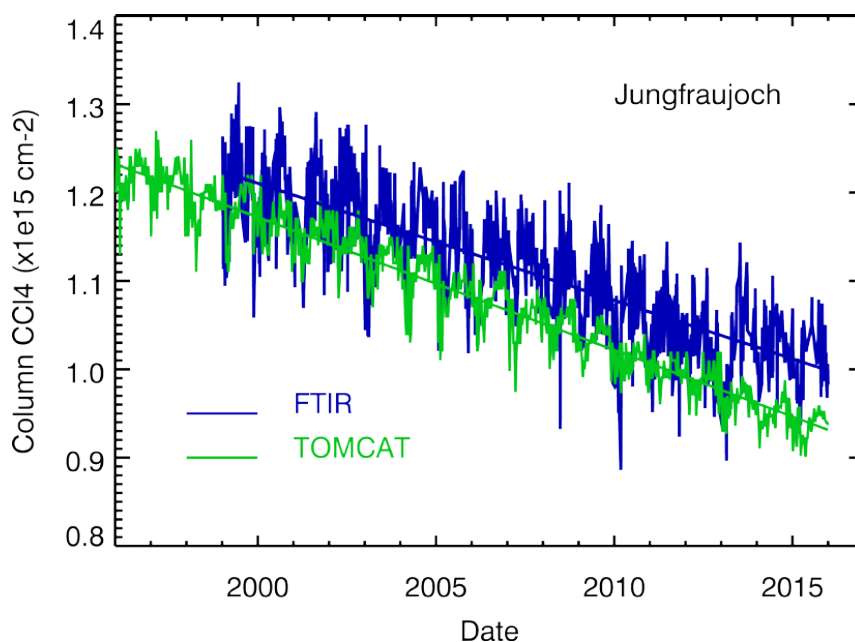
Figure 3. Time series of total column CCl_4 ($\times 10^{15}$ molecules cm^{-2}) at the Jungfraujoch,
NDACC station, Switzerland (46.5ºN, 8ºE) (blue line). The observations have been scaled by
0.9 to account for a possible high bias in the CCl_4 retrieved columns (see Section 3.2). Also
shown are results from model control tracer CTC1 (green line). The straight lines are the
linear fits to the observations and model output.

650
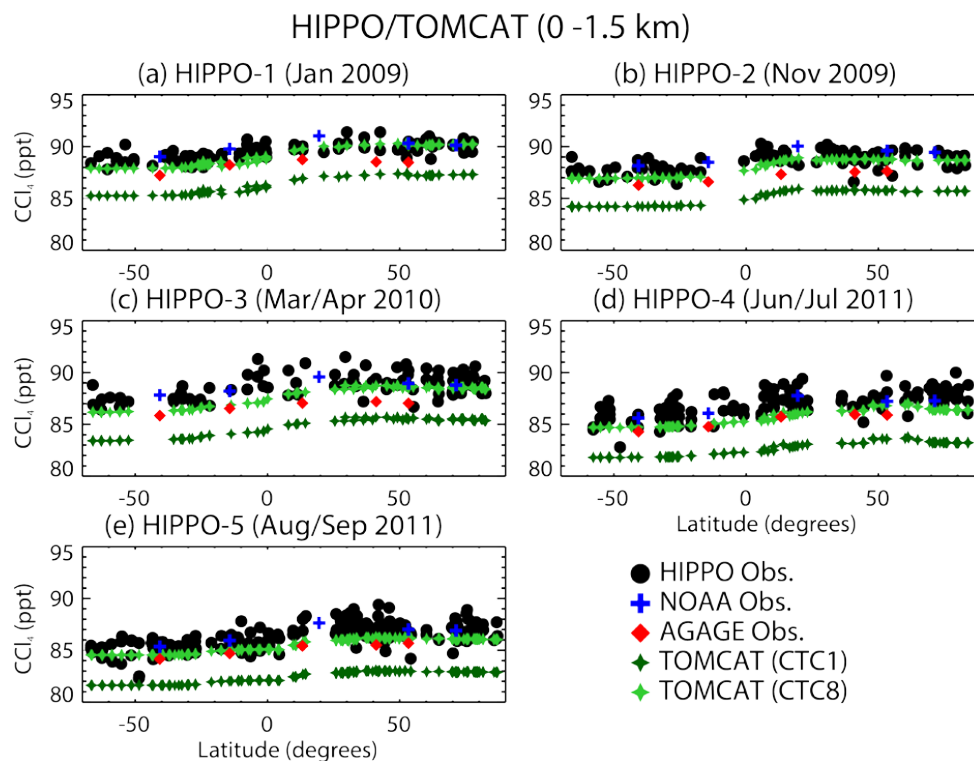
Figure 4. Latitude cross section of HIPPO observations of CCl_4 (ppt, black circles) between the surface and 1.5 km altitude from flights during five campaigns between January 2009 and September 2011. Also shown are mean surface observations from the AGAGE (red diamond) and NOAA (blue +) networks (see **Table 1** and **Figure 2**) for the months of the campaign. Results from model tracers CTC1 and CTC8 are also shown.

Atmospheric
Chemistry
and Physics
Discussions
Open Access
EGU
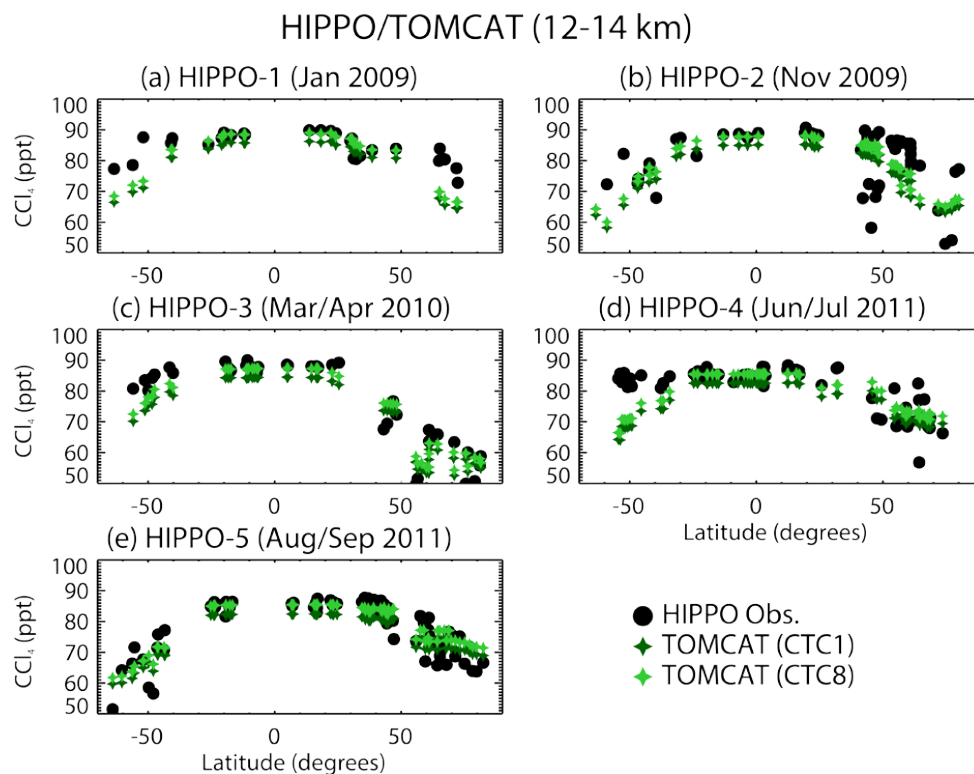
Figure 5. Latitude cross section of HIPPO observations of CCl_4 (ppt, black circles) between 12 and 14 km altitude from flights during five campaigns between January 2009 and September 2011. Results from model tracers CTC1 and CTC8 are also shown.

Atmospheric
Chemistry
and Physics
Discussions

Open Access

663

664
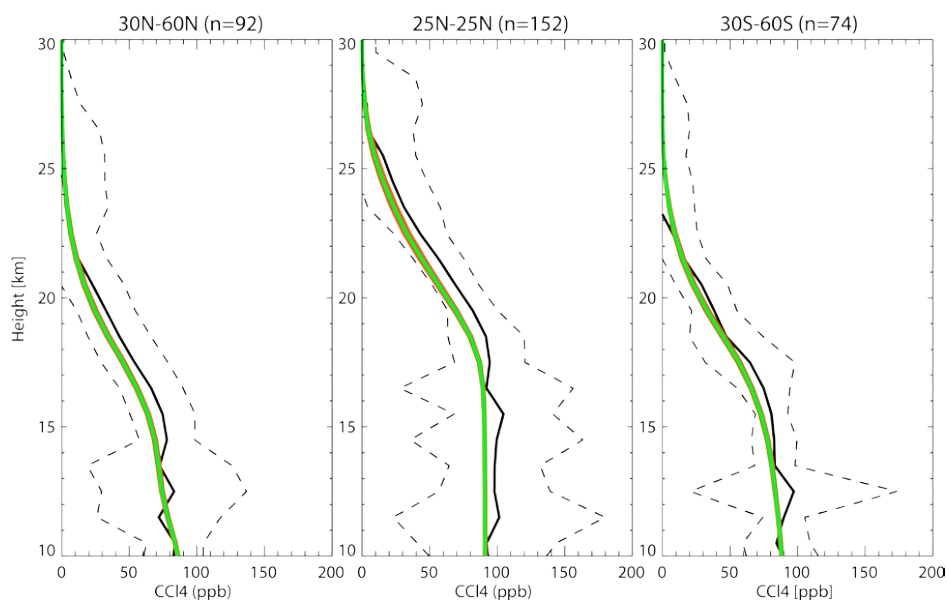
Figure 6. Mean profiles of CCl$_4$ from March-April 2005 as determined from the recent ACE-FTS research retrievals (Harrison et al., 2016) (black line) for latitude bands (a) 30ºN-60ºN, (b) 25ºS-25ºN and (c) 30ºS-60ºS. The number of observed profiles which contribute to the mean is given in the titles (n). The dashed lines show the standard deviation of the observations. Also shown are mean profiles from model control tracer CTC1 for the same latitude bins and time period (green line) and the range of values produced from sensitivity runs CTC6 and CTC7 with ±10% change in CCl$_4$ photolysis rate (orange shading, difficult to see). Note that the model profiles are averages over the indicated spatial regions and are not sampled at the exact locations of the ACE-FTS measurements.

674

Atmospheric
Chemistry
and Physics
Discussions

Open Access

EGU

675

676
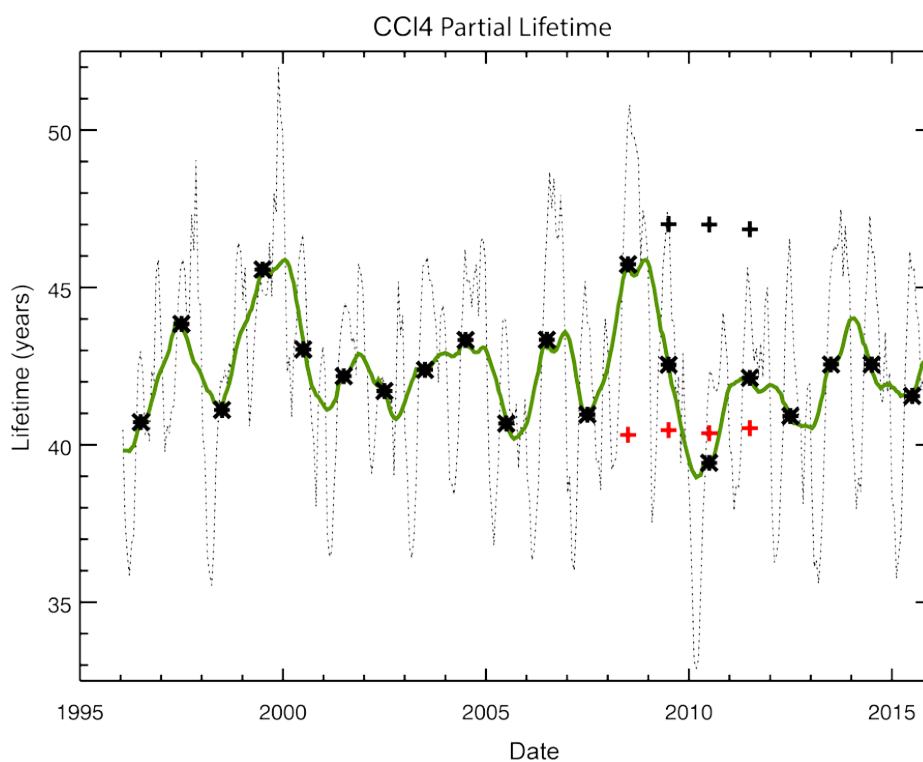
Figure 7. Modelled instantaneous CCl4 partial photolysis lifetime diagnosed from reference
tracer CTC1 (dotted line, value every 20 days) and the same curve with 1-year smoothing
(green solid line). The * symbols indicate the annual mean CCl4 partial lifetime from this
tracer. Also shown are annual mean lifetime results from 4-year simulations (2008-2011)
with repeating winds for 2008 (black +) and 2010 (red +) meteorology.

683

684
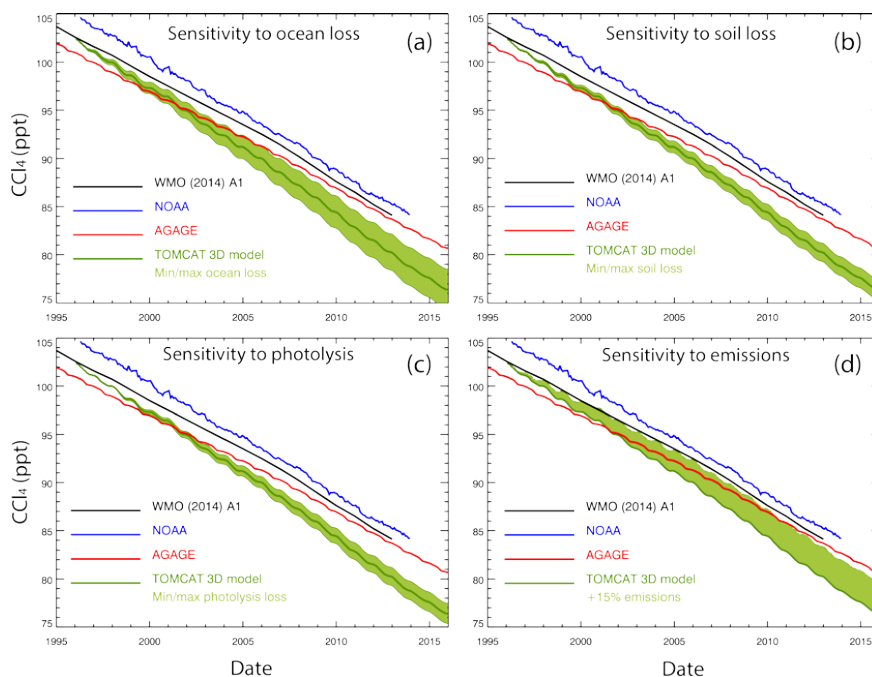
Figure 8. Observed global mean surface CCl₄ from AGAGE (red) and NOAA (blue) networks, along with merged observational dataset from WMO/UNEP (2014) scenario A1 (black line). These are compared with results from TOMCAT model run CTC1 (dark green line) and different sensitivity tracers in each panel with the range given as a light green band: (a) An ocean sink of 157 (tracer CTC2) and 313 (CTC3) years, (b) a soil sink of 298 (CTC4) and 504 (CTC5) years, (c) a ±10% change in stratospheric photolysis (CTC6 and CTC7) and (d) a 15% increase in emissions (CTC8). Note that in panel (d) the light green shading only shows an increase relative to control tracer CTC1 as the sensitivity tracer considered had increased emissions.

695

Atmospheric
Chemistry
and Physics
Discussions

Open Access

EGU

696
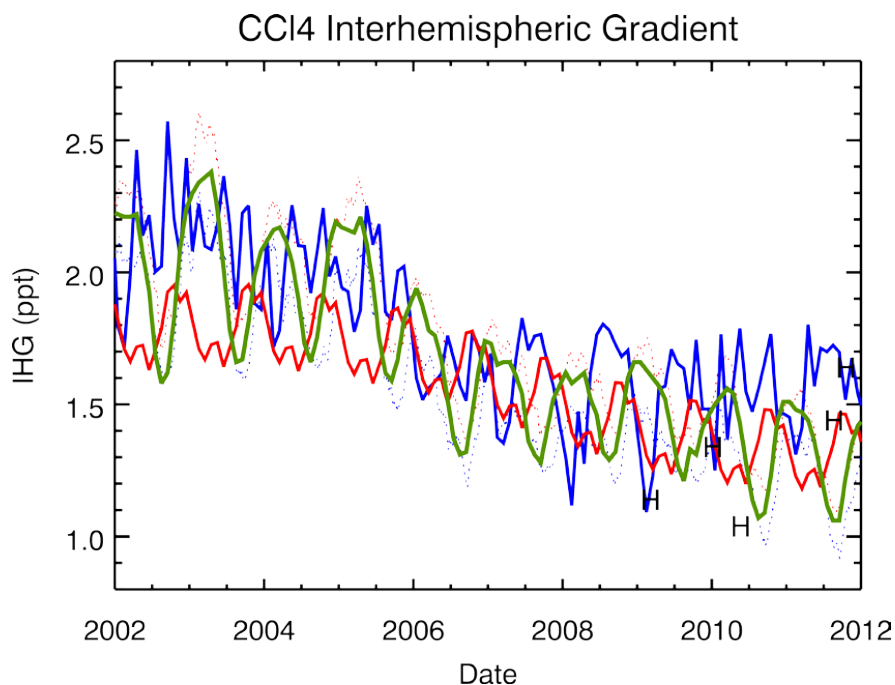
Figure 9. Observed interhemispheric gradient (IHG) of CCl$_4$ (north – south, ppt) from
monthly mean AGAGE (red line) and NOAA (blue line) observations. The NOAA IHG is
estimated by binning the station data by latitude and applying a cosine(latitude) weighting.
The AGAGE IHG is estimated from output of a 12-box model which assimilates the
observations. Also shown are results from the model tracer CTC1 sampled over the whole
model domain (green line), sampled at the AGAGE station locations (red dotted line) and
sampled at the NOAA station locations (blue dotted line). The H symbols show the IHG
estimated from the five HIPPO campaigns (see **Table 3**).